

ESTABLISHING USEFUL SIGNATURES OF LIFE AND HABITABILITY IN THE “SILENT REGION” OF THE RAMAN SPECTRUM.

D. M. Bower^{1,2}, A.C. McAdam², C.S.C. Yang³, T. Hewagama², M. Millan⁴, M.R. Mulholland⁵, U. Udeochu⁶, C. Achilles², C. Knudson^{1,2,7}, J.C. Stern², C.A. Nixon², P.L. Whelley^{1,2,7}

¹University of Maryland, Dept. of Astronomy, College Park, MD, 20742, dina.m.bower@nasa.gov, ²NASA/GSFC, Greenbelt, MD 20771, ³Brimrose Technology Corp., Sparks-Glencoe, MD, 21152, ⁴Laboratoire Atmosphères, Observations Spatiales (LATMOS), LATMOS/IPSL, UVSQ Université Paris-Saclay, Sorbonne Université, CNRS, Guyancourt, France, ⁵Old Dominion University, Norfolk, VA, 23529, ⁶University of the District of Columbia, Washington, DC, 20008, ⁷CRESST II, Greenbelt, MD 20771

Introduction: Life detection in the solar system relies on the unambiguous identification of signatures of life and habitability. Raman spectroscopy is a laser-based vibrational spectroscopy technique capable of identifying organic and inorganic compounds. The NASA Perseverance Rover on Mars utilizes two different Raman spectrometers to characterize the surface environment at Jezero Crater to better understand the habitable potential of Mars [1]. We have explored the use of Raman spectroscopy as a tool to distinguish biotic overprint in secondary sulfate and carbonate formation during field campaigns in analog terrestrial environments [2,3].

The majority of Raman signatures for minerals, organic-biomolecular compounds, and water (H_2O , OH) occur within $\sim 110\text{ cm}^{-1} - 1900\text{ cm}^{-1}$ and $\sim 2500\text{ cm}^{-1} - 3700\text{ cm}^{-1}$ [4,5]. Unfortunately, most natural samples contain mixtures of organic materials and multiple minerals, resulting in overlapping Raman peaks within complicated spectra. An often over looked portion of the Raman spectrum occurs between $\sim 2000\text{ cm}^{-1} - 2400\text{ cm}^{-1}$, mainly because of the luminescence artifacts that can overwhelm this region of the spectrum for certain samples [6]. This region is also known as the “silent region”, since the fingerprint region for most biomolecules and minerals sits outside of this range [7].

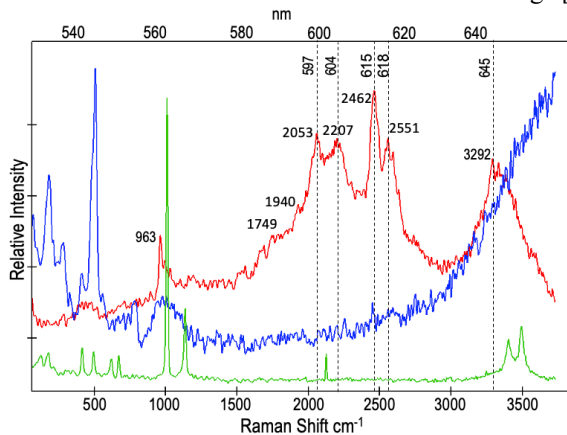


Figure 1. Raman spectrum of a secondary phase gypsum (green) on basalt (blue) showing potential cyanates (isothiocyanate and isocyanate) among phosphatic signatures (red). Upper axis in nm for luminescence.

Raman signatures for cyanates and other nitrogenous compounds are observed within the $\sim 2000\text{ cm}^{-1} - 2300\text{ cm}^{-1}$ region of the spectrum, which sets them apart from the overlapping mineral and organics peaks [8, 9]. Cyanates (e.g., OCN^- or SCN^-) are common in many terrestrial and oceanic biogeochemical systems [10, 11]. Cyanates may have been abundant and essential compounds for metabolisms on early Earth when oxygen levels were low, the environment was reducing, and nitrogen played a key role in the evolution of Earth’s biogeochemical cycle and life [12]. Today on Earth, cyanates can supply nitrogen as well as carbon in terrestrial and marine systems that are otherwise nutrient-limited [13,14]. Extant microbes both produce and consume cyanates, there were ample sources of cyanate compounds likely present on early Earth, and genetic evidence suggests cyanate utilization by early microbes [15]. Nitrogen species have been detected on the surface of Mars, suggesting the potential existence of an ancient nitrogen cycle [16].

Objective: We are investigating the relationships between cyanates, co-occurring organic compounds, and secondary minerals in basaltic environments. Our goal is to establish if these essential components of the nitrogen cycle can serve as unique biosignatures that would be spectroscopically detectable on other planetary bodies.

Methods: We used field-portable Raman spectroscopy with laboratory micro-Raman spectroscopy and spectroscopic imaging in combination with other mission-relevant geochemical techniques to characterize the mineral assemblages, hydrated components, and biomolecules in secondary precipitates and host rocks collected from two different basaltic environments: Hveragil geothermal stream in Iceland and a high-elevation lava tube on Mauna Loa, Hawaii. Field measurements were done using a portable VIS Raman spectrometer (TSI, Inc. EZ Raman), which uses a 532 nm excitation laser with a 1.2 μm fiber optic probe, spot size of 50 μm , spectral range between 100 to 4000 cm^{-1} , and a resolution of $\sim 10\text{ cm}^{-1}$. Calcite (CaCO_3), gypsum ($\text{CaSO}_4 \cdot 2\text{H}_2\text{O}$), and quartz (SiO_2) minerals were used as calibration standards to keep track of any spectrometer drift and to accurately assign

peak positions. Power output was controlled by the instrument software, and a minimum amount of power (0.3 - 2.0 mW) was applied as appropriate for each individual sample. Scan times varied typically ~ 10-40 seconds/spot for each target. Returned samples were probed in the laboratory using the field-portable instrument with the same measurement parameters to acquire additional data. Micro-Raman measurements were done with a WITec α -Scanning Near-Field Optical Microscope customized to incorporate confocal VIS (532 nm) Raman spectroscopy imaging utilizing 50x and 100x objectives to achieve a lateral resolution of ~300 nm and a spot size ~1 μ m. Spectra maps and spot scans were done using low power at the sample (~0.05 - 3 mW) with acquisition times ~1-2 s/pixel for each map and 3-20 seconds/per spot for spot scans. UV-VIS-NIR (UVN, 200 - 1000 nm) + Long-wave IR (LWIR, 5.6 to 10 μ m, 1785 to 1000 cm^{-1} in the mid-IR region) laser induced breakdown spectroscopy (LIBS) was also used in the laboratory to confirm the presence of the cyanates, discern cation variations in the secondary precipitates, and to identify a subset of the organic molecules on the sample surfaces and 3.5 μ m into the samples [17,18]. In addition, Flight-like wet chemistry experiments were also performed on a subset of samples with pyrolysis coupled with MTBSTFA-DMF derivatization, analogous to one of the wet chemistry techniques currently utilized onboard the Sample Analysis at Mars (SAM) instrument of the NASA Curiosity rover [19]. We limited the use of extensive processing of Raman spectra exhibiting high luminescence to avoid introducing user bias and used clean sample handling methods to eliminate potential contamination.

Results and Discussion: The host basalts from both Iceland and Hawaii had similar compositions of plagioclase, pyroxene, and olivine minerals. The dominant secondary precipitates at Hveragil were Ca-carbonates while Ca-, Na-sulfates were predominant in the Mauna Loa lava tube. Similar biomolecular signatures were detected in samples from both Hveragil stream and the Mauna Loa lava tube, including pigments, organic acids, lipids, cyanates, and cyanate-related compounds. Laser-induced luminescence seems to be a potential cause for at least some of the Raman signatures observed in the carbonate samples, likely due to the presence of Mn^{2+} in both the basalts and carbonates. The cyanate signatures in the lava tube samples almost always exclusively occurred with organic phosphorous compounds along with a suite of biomolecules (Fig.1). We do observe a phosphate Raman peak ~ 963 cm^{-1} without the other phosphate mineral bands, so it is possible that this was contributing to the features ascribed to cyanates [20]. Regardless, the LIBS data verified the presence of nitrogenous species in both sample sets (Fig.2).

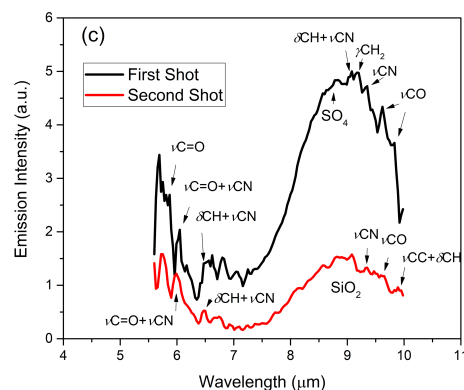


Figure 2. LWIR LIBS depth profiling of gypsum coating on basalt shows multiple organic nitrogen species.

Further Research: We are currently expanding upon our dataset to include other lava tube sites and previously studied oceanic and estuarine systems where cyanate biogeochemistry has been characterized [11,14]. Thin section work has already begun to shed light on the relationships between the secondary minerals, biomolecules, nitrogenous compounds, and phosphorous species. Future work will include Electron Probe Microanalysis (EPMA) and cathode luminescence (CL) to better distinguish cyanates.

Acknowledgments: This work is supported by the NASA Internal Science Funding Model programs Goddard Instrument Field Team (GIFT) and Fundamental Laboratory Research (FLaRe).

References: [1] Farley K. et al. (2020) *Space Sci. Rev.*, 216:142, 1-41. [2] Bower D.M. et al. (2021) *Spec. Chim. Acta A*, 263:120205, 1-14. [3] Bower, D.M. et al. (2022) *AbSciCon, Abs.* 327-04. [4] Czamara K. et al. (2014) *Jour. Raman Spec.*, 46, 4-20. [5] Edwards H.G.M. et al. (2014) *Phil. Trans. R. Soc. A*, 372, 1-12. [6] Moroz T.N. et al. (2021) *Spec. Chim. Acta A*, 250, 1-6. [7] Dodo K. et al. (2022) *Jour. Am. Chem. Soc.*, 144, 19651-19667. [8] Socrates, G. (2001) Wiley. [9] Karaagac, D. (2020) *Bull. Chem. Soc. Ethiop.*, 34(2), 365-376. [10] Mooshamer M. et al. (2021) *Comm. Ear. Env.*, 2(161), 1-10. [11] Widner B. et al. (2017) *Limn. & Ocean.* 62, 2538-2549. [12] Ugelow M. S. et al. (2020) *Astrobiology*, 20(5), 1-12. [13] Palatinszky, M. et al. (2015) *Nature*, 524(7563), 43-44. [14] Widner B. et al. (2016) *Env. Sci. & Tech. Lett.*, 3, 297-302. [15] Mao, X. et al. (2022) *ISME*, 16, 602-605. [16] Stern, J.C. et al. (2015) *PNAS*, 112(14), 4245-4250. [17] Yang, C.S.C. et al. (2022) *Methods X*, 9, 101647, 1-11. [18] Yang, C.S.C. et al. (2017) *Appl. Spec.* 71, 728-734. [19] Mahaffy, P. et al. (2012) *Space Sci. Rev.*, 170, 401-478. [20] Zhukova, I.A. et al. (2021) *Jour. Raman Spec.*, 53, 485-496.